ChemMedChem

Chemistry Europe
European Chemical Societies Publishing

Accepted Article

Title: Synthesis of 2-organylchalcogenopheno[2,3-b]pyridines from elemental chalcogen and NaBH4/PEG-400 as reducing system: antioxidant and antinociceptive properties

Authors: Thiago J. Peglow, Ricardo H. Bartz, Carolina C. Martins, Andrei L. Belladona, Cristiane Luchese, Ethel A Wilhelm, Ricardo Frederico Schumacher, and Gelson Perin

To be cited as: *ChemMedChem* 10.1002/cmdc.202000358

Link to VoR: https://doi.org/10.1002/cmdc.202000358

WILEY-VCH

WILEY-VCH

FULL PAPER

Synthesis of 2-organylchalcogenopheno[2,3-*b*]pyridines from elemental chalcogen and $NaBH_4$/PEG-400 as reducing system: antioxidant and antinociceptive properties

Thiago J. Peglow,[a] Ricardo H. Bartz,[a] Carolina C. Martins,[b] Andrei L. Belladona,[c] Cristiane Luchese,[b] Ethel A. Wilhelm,[b] Ricardo F. Schumacher,*[c] and Gelson Perin*[a]

[a] T. J. Peglow, R. H. Bartz, Prof. G. Perin*
LASOL-CCQFA, Universidade Federal de Pelotas – UFPel
P.O. Box 354 - 96010-900, Pelotas, RS, Brazil.
E-mail: gelson_perin@ufpel.edu.br
[b] C. C. Martins, Prof. C. Luchese, Prof. E. A. Wilhelm
LaFarBio-CCQFA, Universidade Federal de Pelotas – UFPel
96010-900, Pelotas, RS, Brazil
E-mail: ethelwilhelm@yahoo.com.br
[c] A. L. Belladona, Prof. R. F. Schumacher*
CCNE, Universidade Federal de Santa Maria – UFSM
97105-900, Santa Maria, RS, Brazil
E-mail: ricardo.schumacher@ufsm.br

Supporting information for this article is given via a link at the end of the document.

Abstract: An alternative method to prepare 2-organylchalcogenopheno[2,3-*b*]pyridines was developed by the insertion of chalcogen species (selenium, sulfur or tellurium), generated *in situ*, into 2-chloro-3-(organylethynyl)pyridines using the $NaBH_4$/PEG-400 reducing system, followed by an intramolecular cyclization reaction. It was possible to obtain a series of compounds with up to 93% yields in short reaction times. Among the synthesized products, 2-organyltellurophenо[2,3-*b*]pyridines have not been described in the literature so far. Moreover, the compounds 2-phenylthieno[2,3-*b*]pyridine (**3b**) and 2-phenyltellurophenо[2,3-*b*]pyridine (**3c**) exhibited significant antioxidant potential in different *in vitro* assays. Further studies demonstrated that the compound **3b** exerted antinociceptive effect in acute inflammatory and non-inflammatory pain models, indicating the involvement of the central and peripheral nervous system on its pharmacological action. More specifically, our results suggest that the intrinsic antioxidant property of the compound **3b** may contribute to attenuate the nociception and the inflammatory process on the local injury induced by CFA.

Introduction

Chalcogen-containing heterocycles are an important class of compounds that have been extensively exploited in medicinal chemistry[1-3], materials science[4-10] and organic synthesis[11-13]. Among them, chalcogenophenes have presented many promising applications as new materials due to their properties as organic semiconductors, which showed potential as organic field-effect transistors (OFET)[14-19], organic light-emitting diode (OLED)[20-24], and organic solar cells (OSC)[25-31]. In addition, these compounds also have shown promising pharmacological applications[32-37], being found in worldwide consumed drugs[38-42]. Still, chalcogenophenes when associated to another biological active heterocycle, such as pyridine, usually makes the new compound biologically more active[43-47]. Thus, the development of new and efficient methodologies for the synthesis of chalcogenophene-fused pyridine as promising drug candidates is crucial in contemporary organic synthesis. In this sense, many compounds based on thieno[2,3-*b*]pyridine scaffolds have been widely studied[44-49]. For example, Gao and co-workers reported the preparation of the *N*-(thieno[2,3-*b*]pyridine)carboxamide **I** and its evaluation as a target drug for the treatment of autoimmune diseases (Figure 1)[44]. Pevet and co-workers synthesized thieno[2,3-*b*]pyridine-3-amine based drugs **II** which presented potent enzymatic and cellular c-Src inhibition activities[45]. In addition, different thienopyridine derivatives have been described as anticancer **III**[46] and anti-inflammatory agents **IV**[47], among others[48-49].

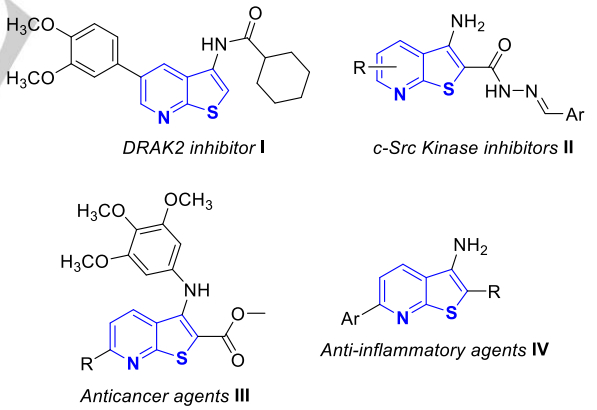

Figure 1. Examples of thieno[2,3-*b*]pyridine-based drug candidates.

Despite the importance of chalcogenophenopyridines, synthetic methodologies for their production remain limited, particularly in the case of selenophene and tellurophene-based compounds. In 2012, Peixoto and co-workers[50] disclosed a method for the synthesis of 2-(hetero)arylthieno[2,3-*b*]- or [3,2-*b*]pyridines by the reaction of 2- or 3-chloro(hetero)arylethynylpyridines with Na_2S (Scheme 1-A). Cai and co-workers[51] described the synthesis of thienopyridines by Pd-catalyzed cross-coupling reaction of *ortho*-fluorinated iodopyridines with terminal alkynes, followed by a thiolation and cyclization process (Scheme 1-B). Recently, our research group described a method to prepare 2-organylselenopheno[2,3-*b*]pyridines starting from bis(3-amino-2-pyridyl) diselenide and aryl- or alkylacetylenes in the presence of ^{t}BuONO as a nitrosating agent[52]. This method was used to synthesize selenopheno[2,3-*b*]pyridine derivatives (Scheme 1-C).

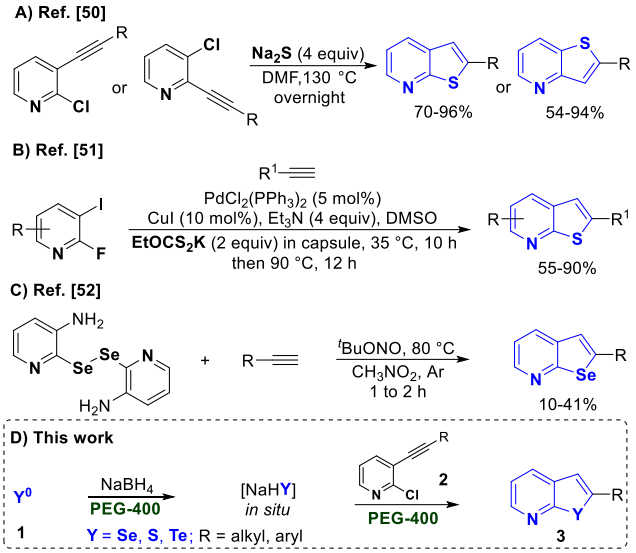

Scheme 1. Previous works on the synthesis of 2-organylchalcogenopheno[2,3-*b*]pyridines and our general protocol.

Due to our continued interest in the synthesis and pharmacological evaluation of organochalcogen compounds, we describe herein an efficient cyclization reaction using elemental chalcogen **1a**-**c** (selenium, sulfur or tellurium) and 2-chloro-3-(organylethynyl)pyridines **2a**-**f** in the presence of $NaBH_4$/PEG-400 as a reducing system for the preparation of new 2-organylchalcogenopheno[2,3-*b*]pyridines **3a**-**r** (Scheme 1-D).

Results and Discussion

Chemistry

Initially, we focused on the optimization of the reaction conditions varying the amount of reagents, temperature and use of eco-friendly solvents. For that, we chosen elemental selenium **1a**, 2-chloro-3-(phenylethynyl)pyridine **2a** and $NaBH_4$ as the standard starting materials. After conducted many experiments, we assumed that the optimal reaction condition to obtain the selenopheno[2,3-*b*]pyridine **3a** consists of two steps as follow: in the first, selenium powder **1a** (0.3 mmol) and $NaBH_4$ (0.9 mmol) are poured into a vessel containing PEG-400 (2.0 mL) under argon atmosphere at 50 °C, and are maintained at this temperature for approximately 0.5 hours. Then, as a second step, 2-chloro-3-(phenylethynyl)pyridine **2a** (0.25 mmol) is added and the temperature is raised to 100 °C stirring for additional 2 hours. The complete optimization of the reaction conditions and their results can be seen on Supporting Information (Table S1).

After completing the optimization tests, to demonstrate the generality of this method, we turned our attention to synthesize a series of 2-organylchalcogenopheno[2,3-*b*]pyridines **3a**-**r** using different elemental chalcogens (selenium, sulfur and tellurium) **1a**-**c** and 2-chloro-3-(organylethynyl)pyridines **2a**-**f** (Table 1). When we conducted reactions using sulfur or tellurium powder, the 2-phenylthieno[2,3-*b*]pyridine **3b** and the 2-phenyltelluropheno[2,3-*b*]pyridine **3c** were obtained in 77% and 45% yield, respectively. It is important to mention that tellurophenо[2,3-*b*]pyridines remained unpublished until now.

In general, sulfur-containing compounds were obtained in higher yields, followed by selenium and tellurium compounds. Still, both electron-donating **3d-i** and electron-withdrawing **3j-l** groups can be present on the aromatic ring without affecting the efficiency of the synthetic methodology. When we focused on thiophenes **3e** and **3h**, a significant increase in the products yield was observed if compared to the non-substituted product **3b**. On the other hand, selenophenes **3d** and **3g**, or tellurophenes **3f** and **3i**, were obtained in similar yields to **3a** and **3c**, respectively. Conversely, we observed that the presence of an electron-withdrawing group disfavored the formation of the chalcogenophene ring **3j** and **3k**. Meanwhile, the tellurophene[2,3-*b*]pyridine **3l** could be obtained in good 66% yield.

Table 1. Reaction scope for synthesis of 2-organylchalcogenopheno[2,3-*b*]pyridines **3a-r**.[a,b]

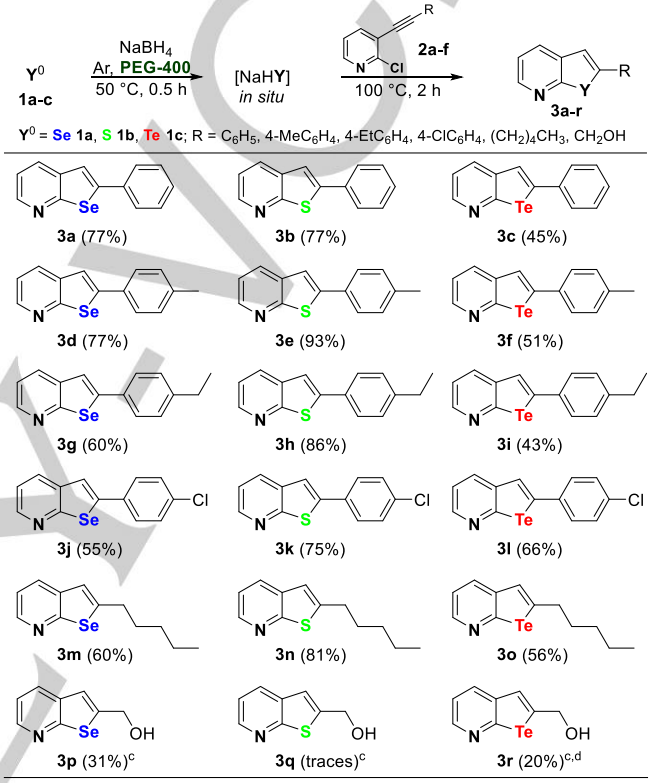

[a] The mixture of the chalcogen **1a-c** (0.3 mmol), $NaBH_4$ (0.9 mmol) and PEG-400 (2.0 mL) was heated to 50 °C and stirred under argon for approximately 0.5 h. After that, the compound **2a-f** (0.25 mmol) was added and the temperature was raised to 100 °C stirring for additional 2 hours. [b] Isolated yield. [c] The reaction remained for 1 hour. [d] Yield is given for ^{1}H NMR analysis.

Furthermore, this protocol also enabled the synthesis of alkyl-substituted chalcogenopheno[2,3-*b*]pyridines **3m**-**o** starting from 2-chloro-3-(heptynyl)pyridine **2e**. In these cases, the reactions occured smoothly and gave the products in yields ranging from 56% to 81%. Finally, the 2-chloropyridine containing a propargyl alcohol group at 3-position (compound **2f**) was also reacted with different elemental chalcogens (Se, S and Te) under the same reaction conditions. The selenopheno[2,3-*b*]pyridin-2-ylmethanol **3p** could be isolated in 31% yield. However, when elemental sulfur was used as reagent a complex mixture of byproducts was obtained and the compound **3q** was observed only in traces amount, while the tellurophenо[2,3-*b*]pyridin-2-ylmethanol **3r** was only confirmed by ^{1}H NMR analysis of a inseparable mixture with 3-(2-chloropyridin-3-yl)propanol. We believe that this byproduct was obtained due to the reduction reaction of the starting material **2e** promoted by $NaBH_4$. The synthesis of **3p-r** were conducted for only 1 hour because we noticed that the prolonged reaction time was involved in byproducts formation.

To complete our investigation and to understand the reaction pathway of the new synthetic methodology, we performed a series of control experiments which can be accessed through the Supporting Information (Scheme S1). Based on these results and

on information from the literature, we also proposed the reaction mechanism outlined in Scheme S2.

Biological evaluation

Different bio-assays were performed to assess the antioxidant properties of the 2-organylchalcogenopheno[2,3-*b*]pyridine compounds **3a-3c**. One of them is based on the overproduction of reactive species (RS), a marker of oxidative damage, by inhibiting one of the electron transport chain enzymes[53]. In this way, the results inserted in Table S2 demonstrated that all the 2-organylchalcogenopheno[2,3-*b*]pyridines **3a-3c** tested were able to reduce the hepatic RS production induced by sodium azide in mice. Despite the compound **3c** exhibited the highest Imax (37.1 ± 4.38) in this assay, it decreased the hepatic RS formation at higher concentrations (100 µM) as well as the compound **3a** (200 µM). On the other hand, the 2-organylchalcogenopheno[2,3-*b*]pyridine **3b**, at all concentrations tested (1 – 500 µM), reduced the RS levels in the liver of mice. Also, the compound **3b** showed similar Imax (18.5 ± 1.04) in this assay than **3a** (19.4 ± 3.22).

The spectrophotometric methods based on pair up the unpaired 2,2'-azino-bis (3-ethylbenzothiazoline-6-sulfonic acid) ($ABTS^+$) and 1,1-diphenyl-2-picrylhydrazyl (DPPH) radicals are widely employed to determine the antioxidant properties of new compounds[54]. According to Table S3, the compounds **3b** and **3c** demonstrated promising effects in scavenging the synthetic radical $ABTS^+$ because they showed similar Imax (86.9 ± 3.84 and 90.0 ± 3.12) to ascorbic acid (99.9 ± 0.05), a widely known antioxidant agent. In special, the 2-organylchalcogenopheno[2,3-*b*]pyridine **3c** exhibited scavenging $ABTS^+$ radical activity at concentrations equal or higher of 10 µM whereas the compound **3b** presented the same effect at higher concentrations (100 µM). In this view, the compound **3c** showed the lowest IC_{50} (31.2 µM ± 0.18), being the most effective among the 2-organylchalcogenopheno[2,3-*b*]pyridines tested in this assay (Table 2). On the other hand, the compound **3b** was able to scavenge DPPH radicals at concentrations ranging from 100 µM to 500 µM, as well as it showed the highest Imax (34.3 ± 2.18) among the compounds tested, being the most promising in this assay. The compound **3c** was able to donate an electron or hydrogen to stabilize the DPPH radical just at higher concentrations (200 µM), as shown in Table S3. The 2-organylchalcogenopheno[2,3-*b*]pyridine **3a**, at all concentrations tested, had no significant difference when compared to control in both $ABTS^+$ and DPPH assays.

Table 2. IC_{50} values of the chalcogenophene compounds **3a-3c** on the $ABTS^+$ radical scavenging.

	Compounds			
	3a	**3b**	**3c**	Ascorbic acid
IC_{50} (µM)	-	155.2 ± 0.03	31.2 ± 0.18	10.8 ± 71.70

Data are expressed as the mean ± SEM. IC_{50} = concentration (µM) to decrease 50% of $ABTS^+$ radical formation.

Furthermore, the pyrogallol autoxidation in an alkaline environment stimulates the release of superoxide radicals in the superoxide dismutase (SOD)-like assay[55]. SODs, superoxide-scavenging enzyme, are already known as the first and most important line of antioxidant enzyme defense system in a cell[56]. In this view, antioxidant compounds that inhibit the pyrogallol autoxidation mimic the SOD function within the cells. The results inserted in Table S4 demonstrated that the 2-organylchalcogenopheno[2,3-*b*]pyridines **3a-3c** had no superoxide-scavenging activity when compared to control. Therefore, our findings suggest that these chalcogenophenopyridines exerted in vitro antioxidant activity throughout mechanisms that do not involve the SOD's function as superoxide scavenger.

Those data clearly indicate that the 2-organylchalcogenopheno[2,3-*b*]pyridine compounds **3a-3c** play as antioxidant agents through multiple mechanisms, mainly by preventing the hepatic RS generation induced by sodium azide. Although both compounds **3b** and **3c** exerted effects as $ABTS^+$ and DPPH radical scavengers, it suggested that their antioxidant activity involve different pathways. In this way, the compound **3c** was the most effective in the $ABTS^+$ assay suggesting that the introduction of the tellurium element enhanced its ability to transfer a pair of electrons to free radicals. On the other hand, the insertion of the sulfur element in the 2-organylchalcogenopheno[2,3-*b*]pyridine **3b** potentiated its ability to donate an electron or hydrogen atom, as shown in the DPPH assay. Regarding the toxicology of organoselenium, organosulfur and organotellurium derivatives, consistent findings have indicated that organotellurium are more toxic than organoselenium compounds[57]. In accordance, a previous study had shown that tellurium pseudopeptides exhibited significant cytotoxic effect in human fibroblast cells when compared to both sulfur and selenium derivatives[58].

Based on our findings and on the toxicology of organochalcogen derivatives, the compound **3b** was chosen to further studies of its pharmacological properties in an acute inflammatory pain model induced by CFA.

A single intraplantar injection of complete Freund's adjuvant (CFA) produces a local immune response which is characterized by the paw edema, vasodilatation and hyperalgesic behavior. Therefore, this animal model is well-recognized for screening novel compounds to acute inflammatory pain[59]. In this view, the Figure 2 illustrated that intraplantar injection of CFA induced a mechanical hyperalgesia in mice. As expected, a single administration of the compound **3b**, at all doses tested, attenuated the mechanical hyperalgesia in CFA-treated mice, suggesting that this 2-organylchalcogenopheno[2,3-*b*]pyridine exhibited an antinociceptive effect. Also, this compound showed pharmacological effect similar to meloxicam (50 mg/kg, ig), a reference drug extensively prescribed in the clinic. However, there is a significant difference on the antinociceptive responses exerted by the 2-organylchalcogenopheno[2,3-*b*]pyridine **3b** and the meloxicam, at the same dose (50 mg/kg), in CFA-treated mice. This finding suggests that the compound **3b** may be more potent than meloxicam.

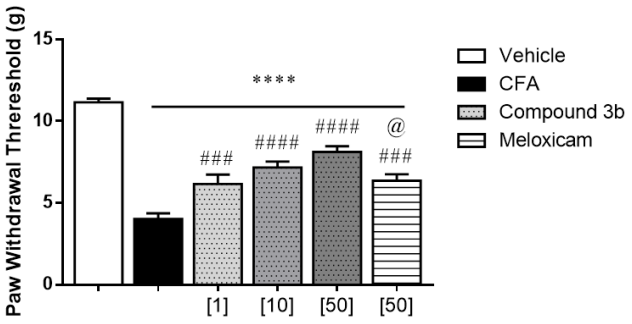

Figure 2: Dose-response of antinociceptive effect of compound **3b** in an acute inflammatory pain model induced by CFA. Each column represents the mean ± S.E.M of 7 mice/group. Asterisks denote the significance levels when compared with the vehicle-treated group: (****) $P < 0.0001$. Hashtags denote the significance levels when compared with the CFA-treated group: (####) $P < 0.0001$ and (###) $P < 0.001$. Arroba denotes the significance levels when compared with compound **3b**-treated group (50 mg/kg): (@) $P < 0.05$ (One-way ANOVA followed by the Newman-Keuls test).

In relation to the time-course antinociceptive effect of the compound **3b**, the Figure 3 demonstrated that the intraplantar injection of CFA triggered a mechanical hyperalgesia in mice which persisted during all experimental period. Indeed, the administration of compound **3b** improved the mechanical stimulus response in CFA-treated mice, that started at 0.5 h and long

lasting up significant until 6 h after the treatment. In a different time profile, meloxicam treatment (50 mg/kg, ig) also reduced the mechanical hyperalgesia in CFA-treated mice. The antinociceptive effect of meloxicam also started at 0.5 h and persisted significant for only 2 h after the administration. In this context, there is an immediate need for new therapeutic approaches as pain management due the low efficacy, the limitations and the adverse effects associated to the analgesic drugs commercially available, including the non-steroidal anti-inflammatory drugs (NSAIDs), the cyclooxygenase-2 (COX-2) selective inhibitors[60] and the opioid drugs[61]. Therefore, our results suggest the compound **3b** may be a promising prototype for the management of acute inflammatory pain conditions.

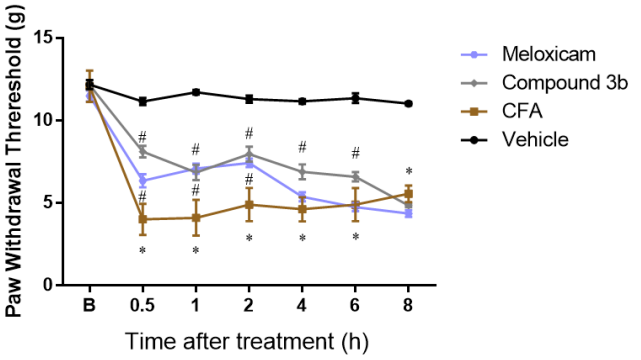

Figure 3. Time-response of antinociceptive effect of compound **3b** in an acute inflammatory pain model induced by CFA. Each column represents the mean ± S.E.M of 7 mice/group. Asterisks denote the significance levels when compared with the vehicle-treated group: (*) P < 0.05. Hashtags denote the significance levels when compared with the CFA-treated group: (#) P < 0.05 (One-way ANOVA followed by the Newman-Keuls test).

It has been well-stablished that the exacerbated production of oxidizing agents is a common feature of inflammatory and painful conditions. Furthermore, the release of inflammatory mediators, including the RS overproduction and the cytokines, sensitizes the nociceptive nerve endings and thus, produces allodynia and hyperalgesia[62]. In this way, we showed that an intraplantar injection of CFA induced the edema formation (Figure 4), as well as increased the RS (Figure 5) and the thiobarbituric acid reactive substances (TBARS) levels in mice (Figure 6).

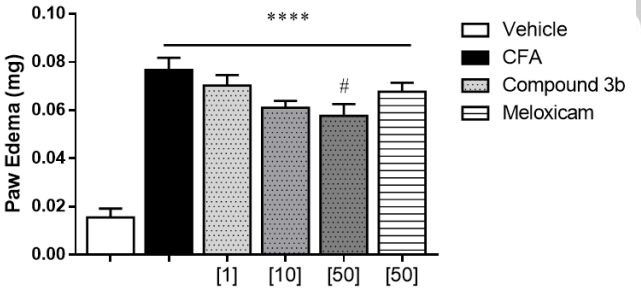

Figure 4. Effect of the acute chalcogenophenopyridine **3b** treatment on the edema formation in mice. Data are expressed as mean ± S.E.M of 7 animals/group. Asterisks denote the significance levels when compared with the vehicle group: (****) P < 0.0001. Hashtags denote the significance levels when compared with CFA-treated group: (#) P < 0.05 (One-way ANOVA followed by the Newman-Keuls test).

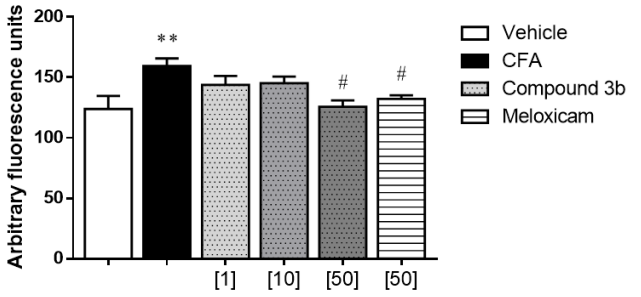

Figure 5. Effect of the acute chalcogenophenopyridine **3b** treatment on the RS levels induced by intraplantar injection of CFA in mice. Data are expressed as mean ± S.E.M of 7 animals/group. Asterisks denote the significance levels when compared with the vehicle group: (**) P < 0.01. Hashtags denote the significance levels when compared with CFA-treated group: (#) P < 0.05 (One-way ANOVA followed by the Newman-Keuls test).

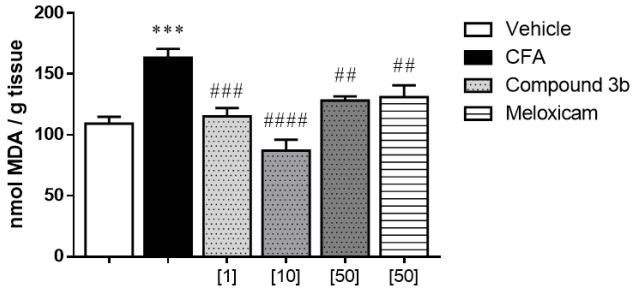

Figure 6: Effect of the acute chalcogenophenopyridine **3b** treatment on the TBARS levels induced by intraplantar injection of CFA in mice. Data are expressed as mean ± S.E.M of 7 animals/group. Asterisks denote the significance levels when compared with the vehicle group: (***) P < 0.001. Hashtags denote the significance levels when compared with CFA-treated group: (####) P < 0.0001, (###) P < 0.001 and (##) P < 0.01 (One-way ANOVA followed by the Newman-Keuls test).

A single administration of the compound **3b**, at all doses tested, reduced the lipidic peroxidation whereas only the highest dose (50 mg/kg, ig) decreased the inflammatory process and the RS levels in the paw of CFA-treated mice. Although the meloxicam did not reduce the edematogenic process, this NSAID drug was effective in decrease the TBARS and RS levels in the paw of CFA-treated mice. In agreement with our findings, previous studies also demonstrated that the meloxicam (10 and 50 mg/kg, ig) was ineffective in reduce the paw edema formation in the formalin and glutamate tests in mice, respectively[63,64]. Despite the difficulties in explain why meloxicam did not reduce the edema formation, it is possible that the selected treatment time (0.5 h) may not be appropriate for this NSAID to inhibit the prostaglandin biosynthesis and thus, exhibits an anti-inflammatory action.

It has been reported that CFA triggers an inflammatory painful condition mediated by the overproduction of free radicals and oxidizing agents[65]. Taken together, these data reinforce the antioxidant properties *in vitro* exerted by the 2-organylchalcogenopheno[2,3-*b*]pyridine **3b**. Moreover, such findings lead us to believe that the compound **3b**, through its free radical-scavenging activity, modulated the oxidative damage and may suppressed the subsequent signaling pathways of inflammation in CFA-treated mice. Consequently, this 2-organylchalcogenopheno[2,3-*b*]pyridine reduced the paw edema as well as the hyperalgesic behavior in mice. Beyond the inflammatory process, it is also known that the intraplantar injection of CFA promotes a sensitization in the central nervous regions related to the pain modulation[66]. Considering the promising effects of the compound **3b** on the CFA-induced inflammatory pain model, we also investigated the involvement of the central nervous system (CNS) on the antinociceptive behavior

exerted by this chalcogenophenopyridine in an acute non-inflammatory nociceptive model, the hot-plate test.
The Figure 7 demonstrated that the compound **3b** (50 mg/kg, ig) enhanced response latency to thermal stimulus when compared with the vehicle group, as well as morphine (50 mg/kg, sc). Indeed, there is a tightly link between the noxious thermal stimulus and the activation of the supraspinal structures sites[67]. In this way, the current finding suggests that the thienopyridine **3b** antinociceptive action may be partially mediated by the CNS signaling. Besides, it was also demonstrated that a single administration of this compound did not alter the number of crossings and rearings when compared to control group.

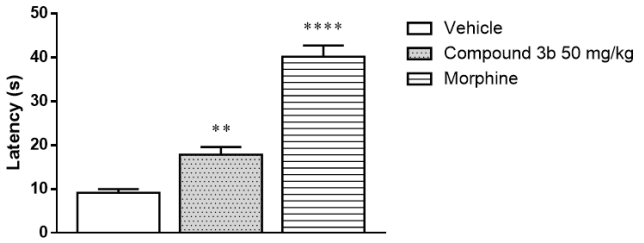

Figure 7. Antinociceptive effect exerted by compound **3b** on the hot plate test. Each column represents the mean ± S.E.M of 7 mice/group. Asterisks denote the significance levels when compared with the control group: (****) $P < 0.0001$ and (**) $P < 0.001$ (One-way ANOVA followed by the Newman Keuls test).

On the other hand, morphine-treated mice increased the number of crossings and decreased the number of rearings when compared to the vehicle group (Table 3). A previous study also showed that a single administration of morphine enhanced the locomotor stimulation in rodents, an adverse effect known as behavior sensitization[68]. The development of this phenomenon, common in most drug of abuses, is highly related to the relapse and drug seeking behavior[69]. Therefore, despite morphine exhibited more potent antinociceptive effect than the compound **3b**, this chalcogenopheno[2,3-*b*]pyridine did not alter the locomotor and exploratory activities, as well as did not induce the locomotor sensitization, a sign of addictive behavior, in mice.

Table 3. Locomotor and exploratory activities of mice treated with thienopyridine **3b** or morphine on the OFT.

Groups	*OFT*	
	Number of crossings	Number of rearings
Vehicle	75.0 ± 3.09	37.3 ± 3.82
Compound **3b**	74.5 ± 5.97	31.3 ± 3.45
Morphine	202.5 ± 21.74****	0.5 ± 0.34****

Data are reported as mean ± S.E.M of 6 mice/group. Statistical analysis was performed using the one-way ANOVA followed by the Newman-Keuls test.

Regarding the toxicity of the 2-phenylthieno[2,3-*b*]pyridine **3b**, this compound appeared to be well tolerated and did not elicit any signs of abnormal behavior or even mortality. In this way, such data were also substantially sustained by the fact that the compound **3b** (50 and 300 mg/kg, ig) did not change the key biochemical parameters of hepatic (aspartate and alanine aminotransferase activities) and renal (urea levels) functions in the plasma of mice (Table 4). Besides, the δ-aminolevulinate dehydratase (δ-ALA-D) activity, a marker sensitive to oxidative stress, as well as RS and TBARS levels were evaluated to determine whether the compound **3b** metabolization deregulates the redox cellular state and thus, the hepatic homeostasis. According to Table 4, a single administration of the compound **3b** (50 and 300 mg/kg, ig) did not alter the oxidative damage parameters in the liver of mice when compared to the vehicle group. Taken together, these findings suggest that the thieno[2,3-*b*]pyridine **3b** appears to have a considerable margin of safety because it has a low toxicity profile in plasma and liver parameters of mice.

Table 4. Effect of a single administration of compound **3b** on the serum and liver toxicological parameters of mice.

	Blood		
	Vehicle	Compound **3b** 50 mg/kg	Compound **3b** 300 mg/kg
AST	16.2 ± 3.39	16.9 ± 3.87	15.1 ± 0.81
ALT	10.4 ± 1.73	10.6 ± 2.62	10.2 ± 1.39
Urea	121.2 ± 8.02	112.8 ± 4.93	109.0 ± 2.46
	Liver		
	Vehicle	Compound **3b** 50 mg/kg	Compound **3b** 300 mg/kg
TBARS	44.9 ± 0.74	41.5 ± 0.73	42.1 ± 2.28
RS	223.9 ± 2.31	216.4 ± 1.18	225.9 ± 4.10
δ-ALA-D	12.9 ± 0.07	11.25 ± 1.48	13.3 ± 1.35

The values of serum AST, ALT and urea levels were expressed as U/l and mg/dl respectively, and the data are reported as mean ± S.E.M of 3 animals/group. Also, the results of hepatic TBARS and RS levels as well as δ-ALA-D activity were expressed as nmol MDA/mg protein, arbitrary fluorescence units and nmol PBG/mg protein/h respectively. The statistical analysis was carried out by one-way ANOVA followed by the Newman-Keuls test.

Conclusion

Summarizing, we have developed a simple and efficient method for the synthesis of 2-organylchalcogenopheno[2,3-*b*]pyridines through the cyclization reaction of 2-chloro-3-(organylethynyl)pyridines mediated by the insertion of nucleophilic chalcogen species (selenium, sulfur and tellurium) obtained by the $NaBH_4$/PEG-400 reducing system. Through this protocol it was possible to obtain seventeen compounds with moderate to excellent yields in short reaction times. By this method it was possible to obtain six tellurophene derivatives which are unknown heterocycles in the literature until now.
In addition, the 2-organylchalcogenopheno[2,3-*b*]pyridines **3b** and **3c** demonstrated promising antioxidant properties *in vitro*. Regarding the toxicology of the chalcogens, the compound **3b** was selected to further studies *in vivo*. In this study, it has been shown that the free radical-scavenging activity exerted by the compound **3b** may be involved in its antinociceptive and anti-edematogenic effects at central and peripheral levels. Thus, our results suggest that the compound **3b** could be an efficient, potent and safe prototype to treat acute painful conditions.

Experimental Section

General materials and methods: The reactions were monitored by TLC carried out on Merk silica gel (60 F_{254}) by using UV light as visualization agent and the mixture between 5% of vanillin in 10% of H_2SO_4 under heating conditions as developing agents. Merck silica gel (particle size 0.040-0.063 mm) was used to flash chromatography. Hydrogen nuclear magnetic resonance spectra (^{1}H NMR) were obtained on Bruker Avance III HD 400 MHz employing a direct broadband probe at 400 MHz. The spectra were recorded in $CDCl_3$ solutions. The chemical shifts are reported in ppm, referenced to tetramethylsilane (TMS) as the internal reference. Coupling constants (*J*) are reported in Hertz. Abbreviations to denote the multiplicity of a particular signal are brs (broad singlet) s (singlet), d

(doublet), dd (doublet of doublet), dt (doublet of triplet) t (triplet), q (quartet), quint (quintet) and m (multiplet). Carbon-13 nuclear magnetic resonance spectra (^{13}C NMR) were obtained on Bruker Avance III HD 400 MHz employing a direct broadband probe at 100 MHz. The chemical shifts are reported in ppm, referenced to the solvent peak of $CDCl_3$ (δ 77.0 ppm). Selenium-77 nuclear magnetic resonance spectra (^{77}Se NMR) were obtained on Bruker Avance III HD 400 MHz employing a direct broadband probe at 76 MHz. The chemical shifts are reported in ppm, using as solvent the $CDCl_3$ and as an internal standard the diphenyl diselenide (δ 463 ppm). Telurium-125 nuclear magnetic resonance spectra (^{125}Te NMR) were obtained on Bruker Avance III HD 400 MHz employing a direct broadband probe at 126 MHz. The chemical shifts are reported in ppm, using as solvent the $CDCl_3$ and as an internal standard the diphenyl ditellurate (δ 422 ppm). The high-resolution electrospray ionization mass spectrometry (ESI-QTOF) analysis were performed on a Bruker Daltonics micrOTOF-Q II instrument in positive mode. The samples were solubilized in HPLC-grade acetonitrile and injected into the APCI source by means of a syringe pump at a flow rate of 5.0 µL min^{-1}. The follow instrument parameters were applied: capillary and cone voltages were set to +3500 V and -500 V, respectively, with a desolvation temperature of 180 °C. For data acquisition and processing, Compass 1.3 for micrOTOF-Q II software (Bruker daltonics, USA) was used. The data were collected in the *m/z* range of 50-1200 at the speed of two scans per second. Low-resolution mass spectra were obtained with a Shimadzu GC-MS-QP2010 mass spectrometer. Melting point (mp) values were measured in a Marte PFD III instrument with a 0.1 °C precision.

General procedure for synthesis of 2-organylchalcogenophene[2,3-*b*]pyridines 3a-r: In a 10.0 mL reaction vial containing Se, S or Te (0.3 mmol) in PEG-400 (2.0 mL) under argon atmosphere was added $NaBH_4$ (0.9 mmol) and the mixture was slowly heated to 50 °C being stirred for 30 min. Then, 2-chloro-3-(organylethynyl)pyridine **2** (0.25 mmol) was added and the temperature was raised to 100 °C. The reaction mixture remained under magnetic stirring for 2 h. Then, water was added (25.0 mL) and the reaction was extracted with ethyl acetate (3x 10.0 mL). The organic phase was separated, dried over $MgSO_4$, and the solvent was evaporated under reduced pressure. The product **3** was isolated by column chromatography using hexane/ethyl acetate (97/3) as eluent.

Spectral data of the products

2-Phenylselenopheno[2,3-*b*]pyridine 3a[52]: Yield: 0.050 g (77%); slightly yellowish solid, m.p: 86-88 °C. ^{1}H NMR ($CDCl_3$, 400 MHz) δ (ppm) = 8.37 (dd, *J* = 4.7 and 1.6 Hz, 1H); 7.88 (dd, *J* = 8.0 and 1.6 Hz, 1H); 7.58-7.55 (m, 2H); 7.49 (s, 1H); 7.37-7.28 (m, 3H); 7.20 (dd, *J* = 8.0 and 4.7 Hz, 1H). ^{13}C{^{1}H} NMR ($CDCl_3$, 100 MHz) δ (ppm) = 164.8, 148.9, 146.0, 137.6, 135.8, 131.9, 129.0, 128.8, 126.9, 120.0, 119.9. DEPT-135 NMR ($CDCl_3$, 100 MHz) δ (ppm) = 146.0 (CH), 131.9 (CH), 129.0 (2x CH), 128.8 (CH), 126.9 (2x CH), 120.0 (CH), 119.9 (CH). ^{77}Se NMR ($CDCl_3$, 76 MHz) δ (ppm) = 533.4. MS (rel. int., %) *m/z*: 259 (100.0), 179 (33.2), 151 (20.6), 115 (5.9), 102 (6.6), 89 (8.0). HRMS (APCI-QTOF) calculated mass for $C_{13}H_9NSe$ $[M^+H]^+$: 259.9978, found: 259.9984.

2-Phenylthieno[2,3-*b*]pyridine (3*b*)[50]: Yield: 0.041 g (77%); yellow solid, m.p: 94-95 °C. ^{1}H NMR ($CDCl_3$, 400 MHz) δ (ppm) = 8.50 (dd, *J* = 4.6 and 1.4 Hz, 1H); 7.97 (dd, *J* = 8.0 and 1.4 Hz, 1H); 7.71-7.69 (m, 2H); 7.44-7.40 (m, 3H); 7.37-7.33 (m, 1H); 7.25 (dd, *J* = 8.0 and 4.6 Hz, 1H). ^{13}C{^{1}H} NMR ($CDCl_3$, 100 MHz) δ (ppm) = 161.4, 146.2, 144.4, 134.2, 133.8, 130.6, 129.0, 128.7, 126.5, 119.7, 116.6. DEPT-135 NMR ($CDCl_3$, 100 MHz) δ (ppm) = 146.2 (CH), 130.6 (CH), 129.0 (2x CH), 128.7 (CH), 126.5 (2x CH), 119.7 (CH), 116.6 (CH). MS (rel. int., %) *m/z*: 211 (100.0), 179 (4.7), 151 (2.3), 115 (1.3), 102 (1.7), 89 (1.7).

2-Phenyltellurophenо[2,3-*b*]pyridine 3c: Yield: 0.035 g (45%); slightly yellowish solid, m.p: 111-112 °C. ^{1}H NMR ($CDCl_3$, 400 MHz) δ (ppm) = 8.40 (dd, *J* = 4.7 and 1.6 Hz, 1H); 7.89 (dd, *J* = 7.9 and 1.6 Hz, 1H); 7.73 (s, 1H); 7.53-7.50 (m, 2H); 7.40-7.31 (m, 3H); 7.27 (dd, *J* = 7.9 and 4.7 Hz, 1H). ^{13}C{^{1}H} NMR ($CDCl_3$, 100 MHz) δ (ppm) = 160.7, 145.9, 145.4, 145.0, 139.4, 133.3, 129.0, 128.5, 127.8, 127.6, 120.4. DEPT-135 NMR ($CDCl_3$, 100 MHz) δ (ppm) = 145.9 (CH), 133.4 (CH), 129.1 (2x CH), 128.6 (CH), 127.9 (CH), 127.7 (2x CH), 120.5 (CH). ^{125}Te NMR ($CDCl_3$, 126 MHz) δ (ppm) = 725.5. MS (rel. int., %) *m/z*: 309 (80.3), 179 (100.0), 151 (40.8), 115 (1.7), 102 (15.0), 89 (7.2). HRMS (APCI-QTOF) calculated mass for $C_{13}H_9NTe$ $[M^+H]^+$: 309.9875, found: 309.9871.

2-(4-Tolyl)selenopheno[2,3-*b*]pyridine 3d[52]: Yield: 0.053 g (77%); yellow solid, m.p: 108-109 °C. ^{1}H NMR ($CDCl_3$, 400 MHz) δ (ppm) = 8.34 (dd, *J* = 4.7 and 1.4 Hz, 1H); 7.85 (dd, *J* = 7.9 and 1.4 Hz, 1H); 7.44-7.42 (m, 3H); 7.19 (dd, *J* = 7.9 and 4.7 Hz, 1H); 7.12 (d, *J* = 8.0 Hz, 2H); 2.29 (s, 3H). ^{13}C{^{1}H} NMR ($CDCl_3$, 100 MHz) δ (ppm) = 164.0, 149.4, 145.1, 139.0, 138.0, 132.8, 132.0, 129.7, 126.8, 120.0, 119.0, 21.2. DEPT-135 NMR ($CDCl_3$, 100 MHz) δ (ppm) = 145.1 (CH), 132.0 (CH), 129.7 (2x CH), 126.8 (2x CH), 120.0 (CH), 119.0 (CH), 21.2 (CH_3). ^{77}Se NMR ($CDCl_3$, 76 MHz) δ (ppm) = 533.6. MS (rel. int., %) *m/z*: 273 (100.0), 192 (26.1), 115 (12.6), 102 (3.7), 89 (7.3). HRMS (APCI-QTOF) calculated mass for $C_{14}H_{11}NSe$ $[M^+H]^+$: 274.0135, found: 274.0134.

2-(4-Tolyl)thieno[2,3-*b*]pyridine 3e: Yield: 0.052 g (93%); yellow solid, m.p: 107-108 °C. ^{1}H NMR ($CDCl_3$, 400 MHz) δ (ppm) = 8.41 (dd, *J* = 4.7 and 1.4 Hz, 1H); 7.91 (dd, *J* = 8.0 and 1.4 Hz, 1H); 7.52 (d, *J* = 8.0 Hz, 2H); 7.31 (s, 1H); 7.19 (dd, *J* = 8.0 and 4.7 Hz, 1H); 7.15 (d, *J* = 8.0 Hz, 2H); 2.30 (s, 3H). ^{13}C{^{1}H} NMR ($CDCl_3$, 100 MHz) δ (ppm) = 160.7, 145.4, 139.0, 134.6, 131.6, 130.8, 129.7, 129.2, 126.4, 119.7, 115.9, 21.2. DEPT-135 NMR ($CDCl_3$, 100 MHz) δ (ppm) = 145.4 (CH), 130.8 (CH), 129.7 (2x CH), 126.4 (2x CH), 119.8 (CH), 115.9 (CH), 21.2 (CH_3). MS (rel. int., %) *m/z*: 225 (100.0), 191 (3.1), 115 (3.9), 102 (1.0), 89 (3.3). HRMS (APCI-QTOF) calculated mass for $C_{14}H_{11}NS$ $[M^+H]^+$: 226.0690, found: 226.0702.

2-(4-Tolyl)tellurophenо[2,3-*b*]pyridine 3f: Yield: 0.041 g (51%); yellow solid, m.p: 129-130 °C. ^{1}H NMR ($CDCl_3$, 400 MHz) δ (ppm) = 8.39 (dd, *J* = 4.7 and 1.6 Hz, 1H); 7.88 (dd, *J* = 7.9 and 1.6 Hz, 1H); 7.70 (s, 1H); 7.42 (d, *J* = 8.0 Hz, 2H); 7.27 (dd, *J* = 7.9 and 4.7 Hz, 1H); 7.19 (d, *J* = 8.0 Hz 2H); 2.37 (s, 3H). ^{13}C{^{1}H} NMR ($CDCl_3$, 100 MHz) δ (ppm) = 160.5, 145.7, 145.6, 145.1, 138.7, 136.7, 133.1, 129.7, 127.5, 127.1, 120.5, 21.2. DEPT-135 NMR ($CDCl_3$, 100 MHz) δ (ppm) = 145.7 (CH), 133.1 (CH), 129.7 (2x CH), 127.5 (2x CH), 127.1 (CH), 120.4 (CH), 21.2 (CH_3). ^{125}Te NMR ($CDCl_3$, 126 MHz) δ (ppm) = 720.8. MS (rel. int., %) *m/z*: 323 (94.8), 192 (100.0), 115 (28.8), 102 (4.7), 89 (13.1). HRMS (APCI-QTOF) calculated mass for $C_{14}H_{11}NTe$ $[M^+H]^+$: 324.0032, found: 324.0038.

2-(4-Ethylphenyl)selenopheno[2,3-*b*]pyridine 3g[52]: Yield: 0.043 g (60%); slightly yellow solid, m.p: 91-93 °C. ^{1}H NMR ($CDCl_3$, 400 MHz) δ (ppm) = 8.44 (dd, *J* = 4.8 and 1.1 Hz, 1H); 7.94 (dd, *J* = 7.9 and 1.1 Hz, 1H); 7.56 (d, *J* = 8.1 Hz, 2H); 7.53 (s, 1H); 7.28-7.24 (m, 3H); 2.69 (q, *J* = 7.6 Hz, 2H); 1.27 (t, *J* = 7.6 Hz, 3H). ^{13}C{^{1}H} NMR ($CDCl_3$, 100 MHz) δ (ppm) = 164.6, 149.1, 145.7, 145.3, 137.8, 133.3, 131.7, 128.5, 126.9, 120.0, 119.2, 28.6, 15.4. DEPT-135 NMR ($CDCl_3$, 100 MHz) δ (ppm) = 145.7 (CH), 131.7 (CH), 128.5 (2x CH), 126.9 (2x CH), 120.0 (CH), 119.2 (CH), 28.6 (CH_2), 15.4 (CH_3). ^{77}Se NMR ($CDCl_3$, 76 MHz) δ (ppm) = 531.7. MS (rel. int., %) *m/z*: 287 (74.8), 272 (100.0), 191 (17.7), 115 (8.9), 102 (8.0), 89 (9.2). HRMS (APCI-QTOF) calculated mass for $C_{15}H_{13}NSe$ $[M^+H]^+$: 288.0291, found: 288.0288.

2-(4-Ethylphenyl)thieno[2,3-*b*]pyridine 3h[51]: Yield: 0.051 g (86%); yellow solid, m.p: 112-113 °C. ^{1}H NMR ($CDCl_3$, 400 MHz) δ (ppm) = 8.49 (dd, *J* = 4.6 and 1.4 Hz, 1H); 7.96 (dd, *J* = 8.0 and 1.4 Hz, 1H); 7.63 (d, *J* = 8.1 Hz, 2H); 7.39 (s, 1H); 7.27-7.23 (m, 3H); 2.68 (q, *J* = 7.6 Hz, 2H); 1.26 (t, *J* = 7.6 Hz, 3H). ^{13}C{^{1}H} NMR ($CDCl_3$, 100 MHz) δ (ppm) = 161.4, 146.0, 145.2, 144.7, 134.3, 131.2, 130.4, 128.5, 126.5, 119.7, 116.0, 28.6, 15.4. DEPT-135 NMR ($CDCl_3$, 100 MHz) δ (ppm) = 146.0 (CH), 130.4 (CH), 128.5 (2x CH), 126.5 (2x CH), 119.7 (CH), 116.0 (CH), 28.8 (CH_2), 15.4 (CH_3). MS (rel. int., %) *m/z*: 239 (77.6), 224 (100.0), 115 (2.6), 102 (1.8), 89 (3.4). HRMS (APCI-QTOF) calculated mass for $C_{15}H_{13}NS$ $[M^+H]^+$: 240.0841, found: 240.0839.

2-(4-Ethylphenyl)telluropheno[2,3-*b*]pyridine 3i: Yield: 0.036 g (43%); slightly yellow solid, m.p: 95-96 °C. ^{1}H NMR ($CDCl_3$, 400 MHz) δ (ppm) = 8.39 (dd, J = 4.7 and 1.5 Hz, 1H); 7.88 (dd, J = 7.9 and 1.5 Hz, 1H); 7.70 (s, 1H); 7.44 (d, J = 8.1 Hz, 2H); 7.27 (dd, J = 7.9 and 4.7 Hz, 1H); 7.22 (d, J = 8.1 Hz, 2H); 2.67 (q, J = 7.6 Hz, 2H); 1.26 (t, J = 7.6 Hz, 3H). $^{13}C\{^1H\}$ NMR ($CDCl_3$, 100 MHz) δ (ppm) = 160.5, 145.7, 145.6, 145.2, 145.1, 136.9, 133.1, 128.5, 127.6, 127.1, 120.4, 28.6, 15.4. DEPT-135 NMR ($CDCl_3$, 100 MHz) δ (ppm) = 145.7 (CH), 133.1 (CH), 128.5 (2x CH), 127.6 (2x CH), 127.1 (CH), 120.4 (CH), 28.6 (CH_2), 15.4 (CH_3). ^{125}Te NMR ($CDCl_3$, 126 MHz) δ (ppm) = 721.5. MS (rel. int., %) *m/z*: 337 (100.0), 322 (89.4), 191 (61.8), 115 (21.7), 102 (13.6), 89 (20.3). HRMS (APCI-QTOF) calculated mass for $C_{15}H_{13}NTe$ $[M^+H]^+$: 338.0188, found: 338.0179.

2-(4-Chlorophenyl)selenopheno[2,3-*b*]pyridine 3j[52]: Yield: 0.040 g (55%); slightly yellow solid, m.p: 91-92 °C. ^{1}H NMR ($CDCl_3$, 400 MHz) δ (ppm) = 8.38 (dd, J = 4.7 and 1.5 Hz, 1H); 7.89 (dd, J = 7.9 and 1.5 Hz, 1H); 7.48-7.45 (m, 3H); 7.31-7.28 (m, 2H); 7.22 (dd, J = 7.9 and 4.7 Hz, 1H). $^{13}C\{^1H\}$ NMR ($CDCl_3$, 100 MHz) δ (ppm) = 164.3, 147.7, 145.7, 137.7, 134.7, 134.2, 132.3, 129.2, 128.0, 120.3, 120.2. DEPT-135 NMR ($CDCl_3$, 100 MHz) δ (ppm) = 145.7 (CH), 132.3 (CH), 129.2 (2x CH), 128.0 (2x CH), 120.3 (CH), 120.2 (CH). ^{77}Se NMR ($CDCl_3$, 76 MHz) δ (ppm) = 536.7. MS (rel. int., %) *m/z*: 295 (43.1), 293 (100.0), 258 (12.9), 213 (19.4), 115 (1.2), 102 (2.7), 89 (5.0). HRMS (APCI-QTOF) calculated mass for $C_{13}H_8ClNSe$ $[M^+H]^+$: 293.9589, found: 293.9579.

2-(4-Chlorophenyl)thieno[2,3-*b*]pyridine 3k[51]: Yield: 0.046 g (75%); yellow solid, m.p: 123-124 °C. ^{1}H NMR ($CDCl_3$, 400 MHz) δ (ppm) = 8.43 (dd, J = 4.7 and 1.5 Hz, 1H); 7.91 (dd, J = 8.0 and 1.5 Hz, 1H); 7.54-7.51 (m, 2H); 7.32-7.28 (m, 3H); 7.20 (dd, J = 8.0 and 4.7 Hz, 1H). $^{13}C\{^1H\}$ NMR ($CDCl_3$, 100 MHz) δ (ppm) = 161.1, 146.2, 143.2, 134.7, 134.2, 132.2, 130.9, 129.2, 127.6, 119.9, 117.0. DEPT-135 NMR ($CDCl_3$, 100 MHz) δ (ppm) = 146.2 (CH), 130.9 (CH), 129.2 (2x CH), 127.6 (2x CH), 119.9 (CH), 117.0 (CH). MS (rel. int., %) *m/z*: 245 (100.0), 213 (2.6), 113 (2.4), 101 (4.1), 89 (1.4). HRMS (APCI-QTOF) calculated mass for $C_{13}H_8NS$ $[M^+H]^+$: 246.0139, found: 246.0158.

2-(4-Chlorophenyl)telluropheno[2,3-*b*]pyridine 3l: Yield: 0.057 g (66%); yellow solid, m.p: 131-132 °C. ^{1}H NMR ($CDCl_3$, 400 MHz) δ (ppm) = 8.34 (dd, J = 4.7 and 1.6 Hz, 1H); 7.87 (dd, J = 7.9 and 1.6 Hz, 1H); 7.66 (s, 1H); 7.38-7.35 (m, 2H); 7.29-7.22 (m, 3H). $^{13}C\{^1H\}$ NMR ($CDCl_3$, 100 MHz) δ (ppm) = 160.3, 145.4, 145.1, 144.6, 137.9, 134.5, 133.8, 129.2, 128.7, 128.1, 120.6. DEPT-135 NMR ($CDCl_3$, 100 MHz) δ (ppm) = 145.4 (CH), 133.8 (CH), 129.2 (2x CH), 128.7 (2x CH), 128.1 (CH), 120.6 (CH). ^{125}Te NMR ($CDCl_3$, 126 MHz) δ (ppm) = 737.3. MS (rel. int., %) *m/z*: 343 (100.0), 213 (84.0), 178 (67.8), 115 (0.2), 102 (4.3), 89 (4.3). HRMS (APCI-QTOF) calculated mass for $C_{13}H_8ClNTe$ $[M^+H]^+$: 343.9486, found: 343.9488.

2-Pentylselenopheno[2,3-*b*]pyridine 3m[52]: Yield: 0.038 g (60%); orange oil. ^{1}H NMR ($CDCl_3$, 400 MHz) δ (ppm) = 8.39 (dd, J = 4.7 and 1.6 Hz, 1H); 7.83 (dd, J = 7.9 and 1.6 Hz, 1H); 7.22 (dd, J = 7.9 and 4.7 Hz, 1H); 7.05 (t, J = 1.1 Hz, 1H); 2.94 (dt, J = 7.3 and 1.1 Hz, 2H); 1.75 (quint, J = 7.3 Hz, 2H); 1.41-1.35 (m, 4H); 0.91 (t, J = 7.3 Hz, 3H). $^{13}C\{^1H\}$ NMR ($CDCl_3$, 100 MHz) δ (ppm) = 164.8, 152.9, 145.1, 136.8, 130.9, 120.9, 119.6, 33.8, 31.3, 31.2, 22.4, 13.9. DEPT-135 NMR ($CDCl_3$, 100 MHz) δ (ppm) = 145.1 (CH), 130.9 (CH), 120.9 (CH), 119.6 (CH), 33.8 (CH_2), 31.3 (CH_2), 31.2 (CH_2), 22.4 (CH_2), 13.9 (CH_3). ^{77}Se NMR ($CDCl_3$, 76 MHz) δ (ppm) = 544.8. MS (rel. int., %) *m/z*: 253 (47.8), 196 (100.0), 116 (59.2), 102 (8.7), 89 (24.4). HRMS (APCI-QTOF) calculated mass for $C_{12}H_{15}NSe$ $[M^+H]^+$: 254.0448, found: 254.0448.

2-Pentylthieno[2,3-*b*]pyridine 3n: Yield: 0.042 g (81%); slightly yellow oil. ^{1}H NMR ($CDCl_3$, 400 MHz) δ (ppm) = 8.44 (dd, J = 4.7 and 1.6 Hz, 1H); 7.87 (dd, J = 8.0 and 1.6 Hz, 1H); 7.21 (dd, J = 8.0 and 4.7 Hz, 1H); 6.90 (t, J = 1.0 Hz, 1H); 2.89 (dt, J = 7.4 and 1.0 Hz, 2H); 1.75 (quint, J = 7.4 Hz, 2H); 1.40-1.36 (m, 4H); 0.91 (t, J = 7.4 Hz, 3H). $^{13}C\{^1H\}$ NMR ($CDCl_3$, 100 MHz) δ (ppm) = 161.5, 147.5, 145.3, 133.6, 129.7, 119.2, 117.7, 31.2, 30.5, 22.3, 13.9. DEPT-135 NMR ($CDCl_3$, 100 MHz) δ (ppm) = 145.3 (CH), 129.7 (CH), 119.2 (CH), 117.7 (CH), 31.2 (2x CH_2), 30.5 (CH_2), 22.3 (CH_2), 13.9 (CH_3). MS (rel. int., %) *m/z*: 205 (35.9), 148 (100.0), 116 (1.6), 102 (2.8), 89 (2.9). HRMS (APCI-QTOF) calculated mass for $C_{12}H_{15}NS$ $[M^+H]^+$: 206.1013, found: 206.1003.

2-Pentyltellurophenо[2,3-*b*]pyridine 3o: Yield: 0.042 g (56%); yellow oil. ^{1}H NMR ($CDCl_3$, 400 MHz) δ (ppm) = 8.35 (dd, J = 4.7 and 1.7 Hz, 1H); 7.76 (dd, J = 7.9 and 1.7 Hz, 1H); 7.25 (t, J = 1.3 Hz, 1H); 7.22 (dd, J = 7.9 and 4.7 Hz, 1H); 2.92 (dt, J = 7.3 and 1.3 Hz, 2H); 1.69 (quint, J = 7.3 Hz, 2H); 1.44-1.33 (m, 4H); 0.91 (t, J = 7.3 Hz, 3H). $^{13}C\{^1H\}$ NMR ($CDCl_3$, 100 MHz) δ (ppm) = 160.3, 150.1, 145.1, 144.0, 132.2, 128.6, 120.1, 37.7, 33.1, 31.2, 22.4, 13.9. DEPT-135 NMR ($CDCl_3$, 100 MHz) δ (ppm) = 145.1 (CH), 132.2 (CH), 128.6 (CH), 120.1 (CH), 37.7 (CH_2), 33.1 (CH_2), 31.2 (CH_2), 22.4 (CH_2), 13.9 (CH_3). ^{125}Te NMR ($CDCl_3$, 126 MHz) δ (ppm) = 721.9. MS (rel. int., %) *m/z*: 303 (36.3), 246 (51.8), 116 (100.0), 102 (10.6), 89 (51.4). HRMS (APCI-QTOF) calculated mass for $C_{12}H_{15}NTe$ $[M^+H]^+$: 304.0345, found: 304.0357.

Selenopheno[2,3-*b*]pyridin-2-ylmethanol 3p: Yield: 0.017 g (31%); yellow oil. ^{1}H NMR ($CDCl_3$, 400 MHz) δ (ppm) = 8.45 (dd, J = 4.7 and 1.6 Hz, 1H); 7.92 (dd, J = 7.9 and 1.6 Hz, 1H); 7.30-7.26 (m, 2H); 4.97 (s, 2H); 2.43 (brs, 1H). $^{13}C\{^1H\}$ NMR ($CDCl_3$, 100 MHz) δ (ppm) = 165.1, 151.0, 145.9, 136.3, 132.0, 120.9, 119.8, 63.1. DEPT-135 NMR ($CDCl_3$, 100 MHz) δ (ppm) = 145.9 (CH), 132.0 (CH), 120.9 (CH), 119.8 (CH), 63.1 (CH_2). ^{77}Se NMR ($CDCl_3$, 76 MHz) δ (ppm) = 539.5. MS (rel. int., %) *m/z*: 213 (61.5), 196 (12.6), 184 (100.0), 116 (20.7), 102 (11.6), 89 (9.0). HRMS (APCI-QTOF) calculated mass for C_8H_7NOSe $[M^+H]^+$: 213.9771, found: 213.9757.

Tellurophenо[2,3-*b*]pyridin-2-ylmethanol 3r: Yield by ^{1}H NMR (20%); yellowish oil. Mixture of compounds **3r** and 3-(2-chloropyridin-3-yl)propanol **3r'** (ratio 4:1, respectively). Asterisk denotes the chemical shifts of the 3-(2-chloropyridin-3-yl)propanol **3r'**. ^{1}H NMR ($CDCl_3$, 400 MHz) δ (ppm) = 8.35 (dd, J = 4.7 and 1.4 Hz, 1H); 8.23* (dd, J = 4.8 and 1.8 Hz, 1H) 7.81 (dd, J = 7.9 and 1,4 Hz, 1H); 7.57* (dd, J = 7.5 and 1.8 Hz, 1H) 7.27-7.24 (m, 1H); 7.16* (dd, J = 7.5 and 4.8 Hz, 1H) 4.92 (s, 2H); 3.71* (t, J = 6.3 Hz, 2H); 3.28 (brs, 1H); 3.28* (brs, 1H); 2.82* (t, J = 7.6 Hz, 2H); 1.94-1.87* (m, 2H). $^{13}C\{^1H\}$ NMR ($CDCl_3$, 100 MHz) δ (ppm) = 160.0, 151.5, 147.2*, 144.9, 144.3, 139.0*, 136.0*, 133.4, 126.3, 122.6*, 120.1, 65.5, 61.7*, 31.8*, 29.4*. DEPT-135 NMR ($CDCl_3$, 100 MHz) δ (ppm) = 147.2* (CH), 144.9 (CH), 139.0* (CH), 133.4 (CH), 126.3 (CH), 122.6* (CH), 120.1 (CH), 65.5 (CH_2), 61.7* (CH_2), 31.8* (CH_2), 29.4* (CH_2). ^{125}Te NMR ($CDCl_3$, 126 MHz) δ (ppm) = 741.8. MS (rel. int., %) *m/z*: 263 (83.2), 246 (2.9), 116 (43.3), 104 (100.0), 89 (28.6). HRMS (APCI-QTOF) calculated mass for C_8H_7NOTe $[M^+H]^+$: 263.9668, found: 263.9653.

Animals

Male Swiss mice (two months old, 25-35 g) were provided by the local breeding colony. The animals were housed in groups with free access to food and water. They were kept in a separate animal room, under a 12-hour light/ 12-hour dark cycle (the lights were turned on at 07.00 a.m), in an appropriate temperature environment (22 ± 2 °C). A commercial diet and filtered water were available ad libittum. The experimental protocol was approved by the Committee on Care and Use of Experimental Animal Resources of the Federal University of Pelotas, Rio Grande do Sul, Brazil, affiliated to the National Council for the Control of Animal Experimentation and registered under the number 1877/2016 and 1287/2016. All procedures were performed according to National Institutes of Health Guide for the Care and Use of Laboratory Animals and every effort was made to minimize both the suffering and the number of animals utilized.

Preparation of tissue homogenate

Samples of paw and liver were homogenized (1:10, w/v) in 50 mM of Tris-HCl at pH 7.4. The homogenates were then centrifuged at 2,500 x g for 10 min at 4ºC and the low-speed supernatant (S_1) was used for in vitro and ex vivo assays.

***In vitro* assays**

Reactive species (RS) assay: The sodium azide, a cytochrome oxidase inhibitor, induces mitochondrial dysfunction and consequently promotes the overproduction of RS levels[57]. The levels of RS were estimated in the liver of mice. The 2-organylchalcogenopheno[2,3-*b*]pyridine compounds were diluted in DMSO and then they were assayed at 1, 10, 100, 200 and 500 µM. In this method, the compounds **3a-3c** were incubated with an aliquot of the supernatant S_1, 10 mM Tris-HCl buffer at pH 7.4 and 1 mM dichloro-dihydro-fluorescein diacetate (DCFH-DA) in the presence or the absence of the 10 mM sodium azide, a pro-oxidant substance, during 1 hour at room temperature (RT) in the dark. The oxidation of DCFH-DA to fluorescent dichlorofluorescein (DCF) is measured for the detection of intracellular RS[73]. The DCF fluorescence intensity was determined at 488 nm for excitation and 520 nm for emission and the results were expressed as the percentage (%) of control.

2,2'-azino-bis (3-ethylbenzothiazoline-6-sulfonic acid) (ABTS) radical scavenging activity assay: In this assay, the long-life radical cation $ABTS^+$ is generated by the oxidation of ABTS with the potassium persulfate. The reduction in the intensity of greenish coloration characteristic of this radical reflects the ability of the antioxidant compounds to donate a hydrogen atom and scavenge the $ABTS^+$ radical[70]. The 2-organylchalcogenopheno[2,3-*b*]pyridine compounds were diluted in dimethyl sulfoxide (DMSO) and then they were assayed at 1, 10, 100, 200 and 500 µM. Briefly, an aliquot of the compounds 3a-3c was mixed with the ABTS solution diluted in a phosphate buffer saline pH 7.4 during 30 minutes at RT in the dark. The ascorbic acid at 1, 10, 100, 200 and 500 µM was used as a positive control to determine the maximal decrease in the $ABTS^+$ absorbance. The color reaction was measured at 734 nm and the results were expressed as percentage (%) of the control.

Diphenyl-1-picryl hydrazyl (DPPH) radical scavenging activity assay: In this method, the stable free radical DPPH could accept an electron or hydrogen radical to become a stable molecule. The free radical scavenging activity of the antioxidant compounds was assessed by the coloration change, from deep purple to yellow, of the DPPH ethanolic solution[71]. The 2-organylchalcogenopheno[2,3-*b*]pyridine compounds were diluted in DMSO and then they were assayed at 1, 10, 100, 200 and 500 µM. Briefly, the DPPH ethanolic solution was mixed with an aliquot of the compounds 3a-3c during 30 minutes at RT in the dark. The ascorbic acid at 1, 10, 100, 200 and 500 µM was used as a reference standard to determine the maximal decrease in the DPPH absorbance. The bleaching of the purple colored ethanol solution of DPPH was measured at 517 nm and the results were expressed as percentage (%) of the control.

Superoxide dismutase (SOD)-like activity assay: The pyrogallol autoxidation at pH 8.5 generates superoxide radicals being responsible for a time-dependent increase in the absorbance at 412 nm. The SOD-like assay was performed to determine the ability of a superoxide radical scavenger to inhibit the autoxidation of the pyrogallol which it is identified as a SOD function[72]. The 2-organylchalcogenopheno[2,3-b]pyridine compounds were diluted in DMSO and then they were assayed at 1, 10, 100, 200 and 500 µM. In this method, an aliquot of the compounds **3a-3c**, 50 mM Tris-HCl buffer at pH 8.5 and pyrogallol were pre-incubated for 10 min at RT in the dark. Then it was incubated with 1N hydrochloric acid. After 10 min under the same conditions, the color reaction was measured at 412 nm and the results were expressed as the percentage (%) of control.

***In vivo* experiments**

Dose-response curve of compound 3b in an acute inflammatory pain model: In attempt to better elucidate the compound **3b** antinociceptive effect *in vivo*, the dose-response curve was carried out in an acute inflammatory pain model induced by CFA. As described by Cunha et al.[74], the mechanical hyperalgesia was defined as the behavioral parameter measured using the electronic anesthesiometer (Insight, Ribeirão Preto, SP, Brazil). For this purpose, the animals were randomly assigned to six groups (n= 7 animals/group).

In this experiment, the animals received a subcutaneous intraplantar CFA injection (1 mg/ml of heat killed *Mycobacterium tuberculosis* in 85% paraffin oil and 15% mannide monoleate, 20 µl) into the right hindpaw and saline solution (0.9%, w/v, 20 µl) into the left hindpaw. Also, mice received vehicle (canola oil, 10 ml/kg), compound **3b** (1, 10 and 50 mg/kg) or meloxicam (50 mg/kg), a positive control, by the ig route 24 h later the CFA injection. The mechanical paw withdrawal threshold was measured before (baseline values) and at 0.5 h after the last treatments administration to evaluate the dose-response curve.
After the behavioral test, the animals were euthanized and both hindpaws were cut at the ankle joint and weighed on an analytical balance. The paw edema was measured by difference between right paw (CFA treatment) and left paw (vehicle treatment) and the results were expressed in mg. The samples of CFA-treated paw were quickly frozen at -20 °C for further biochemical analyses (RS and lipid peroxidation assays).

Time-response curve of compound 3b in an acute inflammatory pain model: The treatment time-curve was conducted with compound **3b** at the dose of 50 mg/kg which was chosen based on the best antinociceptive effect obtained in the dose-response curve. In this experiment, another set of animals were randomly assigned into four groups (n= 7 animals/group). Mice received a subcutaneous intraplantar CFA injection (1 mg/ml of heat killed *Mycobacterium tuberculosis* in 85% paraffin oil and 15% mannide monoleate, 20 µl) into the right hindpaw and saline solution (0.9%, w/v, 20 µl) into the left hindpaw. Also, mice received vehicle (canola oil, ig, 10 ml/kg), compound **3b** (50 mg/kg, ig) or meloxicam (50 mg/kg, ig) 24 h later the CFA injection. The mechanical paw withdrawal threshold was measured before (baseline values) and at 0.5, 1, 2, 4, 6 and 8 h after the last treatments administration to evaluate the time-response curve.

Hot-plate test: The hot-plate test, widely employed as a model of acute non-inflammatory nociception, evaluates the possible central action of new developed compounds with potential antinociceptive properties. In this test, mice were individually placed in a glass cylinder on a heated metallic surface that was maintained at a temperature of 55 ± 1 °C[75]. The time between the animal placement on the hot plate and the reaction to a noxious thermal stimulus (jumping off the surface, licking and shaking of the hind paws) was recorded as the latency to nociceptive response (seconds). It was established a cut-off time of 45 s in attempt to avoid any injury on the animal paws. The thermal withdrawal latency (seconds) for each animal was recorded 0.5 h after the treatment with the compound **3b** (50 mg/kg, ig), vehicle (canola oil, ig) or morphine (50 mg/kg), a positive control, by the subcutaneous (sc) route (n= 6 animals/group). The treatment time was defined in accordance to the best effect obtained in the time-response curve, which was carried out with compound **3b** at 50 mg/kg. To discard any alterations that could be misinterpreted as nociception, the locomotor and exploratory activities of mice were assessed before the hot plate test.

Open field test (OFT): This test evaluates the exploratory behaviors and the general locomotor activity in mice. The apparatus was made of plywood (30 H x 45 L x 45 W) in which the floor was divided into 9 squares (3 rows of 3) by masking tape markers. Thirty minutes after the treatments, each animal was placed at the center of the open field and observed for 4 min. The locomotor (number of segments crossed with the four paws) and exploratory (number of rearings) activities were recorded during 4 min[76]. The arena was cleaned with 30% ethanol after each session.

Acute oral toxicity studies: In order to explore the toxicological effects of the compound **3b**, another group of mice (n= 3 animals/group) received a single dose of the 2-phenylthieno[2,3-*b*]pyridine **3b** (50 and 300 mg/kg, ig) or vehicle (canola oil). Thus, these animals were observed for up to 72 h to determine the lethal potential of this compound. After this time of exposure, mice were anesthetized to blood collection by heart puncture for further biochemical markers analysis of liver and kidney functions. The

aspartate (AST) and alanine aminotransferase (ALT) activities as well as the urea levels in the plasma were determined by colorimetric tests. AST and ALT activities were expressed as units (U)/l and urea levels were expressed as mg/dl. The samples of liver were also collected to determine TBARS and RS levels, as well as δ-ALA-D activity.

***Ex vivo* studies**

Lipid peroxidation assay (TBARS method): TBARS assay was performed to indirectly determine the malondialdehyde (MDA) levels, an important lipid peroxidation marker. As previously described by Ohkawa et al.[77], MDA reacts with 2-thiobarbituric acid (TBA) under acidic conditions and high temperatures to yield the chromogen. The S_1 aliquots were incubated with 0.8% TBA, acetic acid buffer (pH 3.4) and 8.1% sodium dodecyl sulfate (SDS) for 2 h at 95 °C. The color reaction was measured at 532 nm and the results were expressed as nmol of MDA/mg of tissue.

RS assay: An aliquot of 1 mM DCHF-DA in ethanol was incubated with the supernatant S_1 and 10 mM Tris-HCl buffer at pH 7.4 for 1h at RT in the dark. DCHF-DA, easily oxidized to DCF, is used as fluorescent probe to detect RS levels. Thus, the oxidation of DCHF-DA into DCF was determined at 488 nm for excitation and 525 nm for emission. DCF fluorescence intensity was expressed as arbitrary fluorescence intensity.

Estimation of δ-ALA-D activity: Described by Sassa[78], δ-ALA-D activity was estimated by the rate of product porphobilinogen (PGB) formation. The supernatant S_1 was preincubated with 1 M potassium phosphate buffer pH 6.8 for 10 min at 37 °C. The enzymatic reaction was initiated by adding the substrate (δ-ALA) and the mixture was incubated for 1 h at 37 °C. The reaction was stopped with 10% TCA solution with 10 mM HgCl2. The color of the product reaction was measured at 555 nm using Ehrlich's modified reagent. The values were expressed as nmol PGB/mg protein/h.

Bradford method of protein estimation: The protein concentration was estimated according to the method described by Bradford[79], using a bovine serum albumin (1 mg/ml) as a standard. The color was measured spectrophotometrically at 595 nm.

Statistical analysis

The results were reported as mean ± standard error of the mean (S.E.M). The D'Agostino and Pearson omnibus tests were used to test a Gaussian distribution of the data. Then, these data were analyzed by the one-way analyses of variance (ANOVA) followed by the post-hoc Newman-Keuls test when appropriate. All analyses of the results were performed using GraphPad Prism 6.0 software (San Diego, CA, USA). Probability value of $P < 0.05$ was considered statistically significant. The IC_{50} values were calculated from the graph of the radical-scavenging effect percentage versus the compound concentration. The percentage (%) of maximal inhibition (Imax) was obtained by the absorbances difference between the most effective concentration of the compounds in each assay in relation to negative control.

Acknowledgements

The authors thank the Fundação de Amparo à Pesquisa do Estado do Rio Grande do Sul (FAPERGS) (PqG 19/2551-0001867-3), Conselho Nacional de Desenvolvimento Científico e Tecnológico (CNPq) and Financiadora de Inovação e Pesquisa (FINEP) for the financial support. CNPq is also acknowledged for the fellowships to EAW and GP. This study was financed in part by the Coordenação de Aperfeiçoamento de Pessoal de Nível Superior - Brasil (CAPES) - Finance Code 001.

Keywords: antinociception • antioxidant • chalcogen • chalcogenophenopyridine • green solvent

[1] D. Gramec, L.P. Mašič, M.S. Dolenc, *Chem. Res. Toxicol*. **2014,** *27***,** 1344-1358.
[2] M. Pieroni, E. Azzali, N. Basilico, S. Parapini, M. Zolkiewski, C. Beato, G. Annunziato, A. Bruno, F. Vacondio, G. Costantino, *J. Med. Chem*. **2017**, *60*, 1959-1970.
[3] L. Berrade, B. Aisa, M.J. Ramirez, S. Galiano, S. Guccione, L.R. Moltzau, F.O. Levy, F. Nicoletti, G. Battaglia, G. Molinaro, I. Aldana, A. Monge, S. Perez-Silanes, *J. Med. Chem*. **2011**, *54*, 3086-3090.
[4] L. Fan, G. Chen, L. Jiang, J. Yuan, Y. Zou, *Chem. Phys*. **2017**, *493*, 77-84.
[5] D. Zhang, M. Wang, X. Liu, J. Zhao, *RSC Adv*. **2016**, *6*, 94014-94023.
[6] T. Ma, Q. Zhao, J. Wang, Z. Pan, *J. Chen, Chem. Int*. **2016**, *55*, 6428-6432.
[7] A. Cetin, C. Istanbulluoglu, S.O. Hacioglu, S.C. Cevher, L. Toppare, A. Cirpan, *J. Polym. Sci., Part A: Polym. Chem.* **2017**, *55*, 3705-3715.
[8] Y.-C. Pao, C.-T. Yang, Y.-Y. Lai, W.-C. Huang, C.-S. Hsu, Y.-J. Cheng, *Polym. Chem*. **2016**, *7*, 4654-4660.
[9] T. Oyama, Y.S. Yang, K. Matsuo, T. Yasuda, *Chem. Commun*. **2017**, *53*, 3814-3817.
[10] W. Xu, M. Wang, Z. Ma, Z. Shan, C. Li, H. Wang, *J. Org. Chem*. **2018**, *83*, 12154-12163.
[11] D.B. Lima, F. Penteado, M.M. Vieira, D. Alves, G. Perin, C. Santi, E.J. Lenardão, *Eur. J. Org. Chem*. **2017**, 3830-3836.
[12] A. Skhiri, R.B. Salem, J.-F. Soulé, H. Doucet, *ChemCatChem*. **2017**, *9*, 2895-2913.
[13] G. Perin, L.K. Soares, P.S. Hellwig, M.S. Silva, J.S.S. Neto, J.A. Roehrs, T. Barcellos, E.J. Lenardão, *New J. Chem*. **2019**, *43*, 6323-6331.
[14] C. Wang, H. Dong, W. Hu, Y. Liu, D. Zhu, *Chem. Rev*. **2012**, *112*, 2208-2267.
[15] B. Kang, W.H. Lee, K. Cho, *ACS Appl. Mater. Interfaces* **2013**, *5*, 2302-2315.
[16] M.R. Reddy, H. Kim, C. Kim, S. Seo, *Synth. Met.* **2018**, *235*, 153-159.
[17] N.C. Mamillapalli, S. Vegiraju, P. Priyanka, C.-Y. Lin, X.-L. Luo, H.-C. Tsai, S.-H. Hong, J.-S. Ni, W.-C. Lien, G. Kwon, S.L. Yau, C. Kim, C.-L. Liu, M.-C. Chen, *Dyes Pigm.* **2017**, *145*, 584-590.
[18] X. Zhou, N. Ai, Z.-H. Guo, F.-D. Zhuang, Y.-S. Jiang, J.-Y. Wang, J. Pei, *J. Chem. Mater*. **2015**, *27*, 1815-1820.
[19] S.M. Lee, H.R. Lee, G.K. Dutta, J. Lee, J.H. Oh, C. Yang, *Polym. Chem*. **2019**, *10*, 2854-2862.
[20] J.E. Anthony, *Chem. Rev*. **2006**, *106*, 5028-5048.
[21] A.R. Murphy, J. M. J. Fréchet, *Chem. Rev*. **2007**, *107*, 1066-1096.
[22] N.T. Kalyani, S.J. Dhoble, *Renewable Sustainable Energy Rev.* **2012**, *16*, 2696-2723.
[23] G.M. Farinola, R. Ragni, *Chem. Soc. Rev*. **2011**, *40*, 3467-3482.
[24] Y. Im, S.Y. Byun, J.H. Kim, D.R. Lee, C.S. Oh, K.S. Yook, J.Y. Lee, *Adv. Funct. Mater*. **2017**, *27*, 1603007-1603031.
[25] Y.-J. Cheng, S.-H. Yang, C.-S. Hsu, *Chem. Rev.* **2009**, *109*, 5868-5923.
[26] C.J. Brabec, M. Heeney, I. McCulloch, J. Nelson, *Chem. Soc. Rev*. **2011**, *40*, 1185-1199.
[27] W.-H. Chang, L. Meng, L. Dou, J. You, C.-C. Chen, Y.M. Yang, E.P. Young, G. Li, Y. Yang, *Macromolecules* **2015**, *48*, 562-568.
[28] G. Chen, S. Liu, J. Xu, R. He, Z. He, H.-B. Wu, W. Yang, B. Zhang, Y. Cao, *ACS Appl. Mater. Interfaces* **2017**, *9*, 4778-4787.
[29] Y.S. Park, T.S. Kale, C.-Y. Nam, D. Choi, R.B. Grubbs, *Chem. Commun.* **2014**, *50*, 7964-7967.
[30] D. He, L. Qiu, J. Yuan, Z.-G. Zhang, Y. Li, Y. Zou, *Polymer* **2017**, *114*, 348-354.
[31] Y. Gao, A. Saparbaev, Y. Zhang, R. Yang, F. Guo, Y. Yang, L. Zhao, *Dyes Pigm.* **2017**, *146*, 543-550.
[32] A.B.A. Mahmoud, G. Kirsch, E. Peagle, *Curr. Org. Synth*. **2017**, *14*, 1091-1101.
[33] K. Chand, Rajeshwari, A. Hiremathad, M. Singh, M.A. Santos, R.S. Keri, *Pharmacol. Rep.* **2017**, *69*, 281-295.
[34] H. Khanam, Shamsuzzaman, *Eur. J. Med. Chem*. **2015**, *97*, 483-504.

[35] R.S. Keri, K. Chand, S. Budagumpi, S.B. Somappa, S.A. Patil, B.M. Nagaraja, *Eur. J. Med. Chem*. **2017**, *138*, 1002-1033.
[36] E. Paegle, I. Domracheva, B. Turovska, M. Petrova, I. Kanepe-Lapsa, A. Gulbe, E. Liepinsh, P. Arsenyan, *Chem. - Asian J*. **2016**, *11*, 1929-1938.
[37] P. Arsenyan, E. Paegle, I. Domracheva, A. Gulbe, I. Kanepe-Lapsa, I. Shestakova, *Eur. J. Med. Chem*. **2014**, *87*, 471-483.
[38] M.-H. H. Lee, G.G. Graham, K.M. Williams, R.O. Day*, Drug Saf*. **2008**, *31*, 643-465.
[39] G.L. Plosker, *Drugs* **2009**, *69*, 2477-2499.
[40] P.L. McCormack, *Drugs* **2015**, *75*, 1915-1923.
[41] M. Vamos, S.H. Hohnloser, *Trends Cardiovasc. Med.* **2016**, *26*, 597-602.
[42] A. Rickli, S. Kopf, M.C. Hoener, M.E. Liechti, *J. Pharmacol*. **2015**, *172*, 3412-3425.
[43] E. Vitaku, D.T. Smith, J.T. Njardarson, *J. Med. Chem*. **2014**, *57*, 10257-10274.
[44] L.-J. Gao, S. Kovackova, M. Šála, A.T. Ramadori, S.D. Jonghe, P. Herdewijn, *J. Med. Chem*. **2014**, *57*, 7624-7643.
[45] I. Pevet, C. Brulé, A. Tizot, A. Gohier, F. Cruzalegui, J.A. Boutin, S. Goldstein, *Bioorg. Med. Chem*. **2011**, *19*, 2517-2528.
[46] R. Romagnoli, P.G. Baraldi, M.K. Salvador, D. Preti, M.A. Tabrizi, M. Bassetto, A. Brancale, E. Hamel, I. Castagliuolo, R. Bortolozzi, G. Basso, G. Viola, *J. Med. Chem*. **2013**, *56*, 2606-2618.
[47] H. Liu, Y. Li, X.-Y. Wang, B. Wang, H.-Y. He, J.-Y. Liu, M.-L. Xiang, J. He, X.-H. Wu, L. Yang, *Bioorg. Med. Chem. Lett*. **2013**, *23*, 2349-2352.
[48] J.W. Lockman, M.D. Reeder, K. Suzuki, K. Ostanin, R. Hoff, L. Bhoite, H. Austin, V. Baichwal, J.A. Willardsen, *Bioorg. Med. Chem. Lett*. **2010**, *20*, 2283-2286.
[49] J.M. Hung, H.J. Arabshahi, E. Leung, J. Reynisson, D. Barker, *Eur. J. Med. Chem*. **2014**, *86*, 420-437.
[50] D. Peixoto, A. Begouin, M.-J.R.P. Queiroz, *Tetrahedron* **2012**, *68*, 7082-7094.
[51] J. Cai, S. Huang, R. He, L. Chen, D. Chen, S. Jiang, B. Li, Y. Li, *Org. Biomol. Chem*. **2017**, *15*, 333-337.
[52] G. Perin, T.J. Peglow, R.H. Bartz, R. Cargnelutti, E.J. Lenardão, R.F. Schumacher, *Arkivoc* **2019**, *2*, 50-64.
[53] Q. Chen, E.J. Vazquez, S. Moghaddas, C.L. Hoppel, E.J. Lesnefsky, *J. Biol. Chem*. **2003**, *278*, 36027-36031.
[54] I. Gülçin, *Chem. Biol. Interact*. **2008**, *179*, 71-80.
[55] I. Semsei, K. Nagy, I. Zs.-Nagy, *Arch. Gerontol. Geriatr*. **1990**, *11*, 187-197.
[56] A.K. Holley, L. Miao, D.K. St. Clair, W.H. St. Clair, *Antioxid. Redox Signaling* **2014**, *20*, 1567-1589.
[57] C.W. Nogueira, G. Zeni, J.B.T. Rocha, *Chem. Rev*. **2004**, *104*, 6255-6285.
[58] S. Shaaban, F. Sasse, T. Burkholz, C. Jacob, *Bioorg. Med. Chem.* **2014**, *22*, 3610-3619.
[59] K. Ren, R. Dubner, *ILAR J*. **1999**, *40*, 111-118.
[60] J. Braun, X. Baraliakos, T. Westhoff, *Semin. Arthritis Rheum*. **2020**, *50*, 285-288.
[61] M.R. Hutchinson, Y. Shavit, P.M. Grace, K.C. Rice, S.F. Maier, L.R. Watkins, *Pharmacol. Rev*. **2011**, *63*, 772-810.
[62] D. Salvemini, J.W. Little, T. Doyle, W.L. Neumann, *Free Radical Biol. Med*. **2011**, *51*, 951-966.
[63] F.S.S. Sousa, R.G. Anversa, P.T. Birmann, M.N. de Souza, R. Balaguez, D. Alves, C. Luchese, E.A. Wilhelm, L. Savegnago, *Pharmacol. Rep.* **2017**, *69*, 871-877.
[64] E.A. Wilhelm, P.S. Soares, A.S. Reis, A. Barth, B.G. Freitas, K.P. Motta, B.B. Lemos, A.G. Vogt, C.A.R. da Fonseca, D.R. Araujo, A.M. Barcellos, G. Perin, C. Luchese, *Pharmacol. Rep.* **2019**, *71*, 1201-1209.
[65] F.A. Pinho-Ribeiro, M.S.N. Hohmann, S.M. Borghi, A.C. Zarpelon, C.F.S. Guazelli, M.F. Manchope, R. Casagrande, W.A. Verri, *Chem. Biol. Interact*. **2015**, *228*, 88-99.
[66] M. Barrot*, Neuroscience* **2012**, *211*, 39-50.
[67] J. Scholz, C.J. Woolf, *Nat. Neurosci*. **2002**, *5*, 1062-1067.
[68] E.A.V. Marinho, A.J. Oliveira-Lima, R. Santos, A.W. Hollais, M.A. Baldaia, R. Wuo-Silva, T.S. Yokoyama, A.L. Takatsu-Coleman, C.L. Patti, B.M. Longo, L.F. Berro, R. Frussa-Filho, *Prog. Neuro-Psychopharmacol. Biol. Psychiatry* **2015**, *58*, 22-31.
[69] J.D. Steketee, P.W. Kalivas, *Pharmacol. Rev*. **2011**, *63*, 348-365.
[70] A. Karadag, B. Ozcelik, S. Saner, *Food Anal. Methods* **2009**, *2*, 41-60.
[71] S.B. Kedare, R.P. Singh, *J. Food Sci. Technol*. **2011**, *48*, 412-422.
[72] S. Marklund, G. Marklund, *Eur. J. Biochem*. **1974**, *47*, 469-474.
[73] S.L. Hempel, G.R. Buettner, Y.Q. O'Malley, D.A. Wessels, D.M. Flaherty, *Free Radical Biol. Med*. **1999**, *27*, 146-159.
[74] G.G. Vivancos, W.A. Verri, T.M. Cunha, I.R.S. Schivo, C.A. Parada, F.Q. Cunha, S.H. Ferreira, *Braz. J. Med. Biol. Res.* **2004**, *37*, 391-399.
[75] G. Woolfre, A.D. MacDonald, *J. Pharmacol. Exp. Ther*. **1944**, *80*, 300-307.
[76] R.N. Walsh, R.A. Cummins, *Psychol. Bull*. **1976**, *83*, 482-504.
[77] H. Ohkawa, N. Ohishi, K. Yagi*, Anal. Biochem*. **1979**, *95*, 351-358.
[78] S. Sassa, *Enzyme* **1982**, *28*, 133-143.
[79] M.M. Bradford, *Anal. Biochem*. **1976**, *72*, 248-254.

10.1002/cmdc.202000358

WILEY-VCH

FULL PAPER

Key Topic: 2-Organylchalcogenopheno[2,3-*b*]pyridines: Synthesis and Biological Evaluation

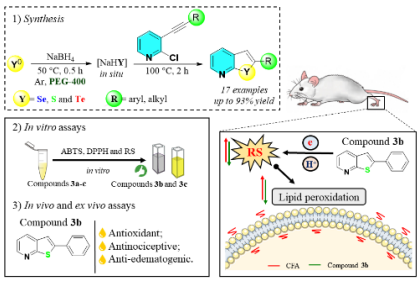

The synthesis of 2-organylchalcogenopheno[2,3-*b*]pyridines was promoted by chalcogen/$NaBH_4$/PEG-400 system. These compounds were obtained in moderated to good yields. Among the synthesized products, the compound **3b** exhibited promising antinociceptive effect in different animal models probably due to its intrinsic antioxidant property.

Institute and/or researcher Twitter usernames: